

AUTOMATED NEURON MORPHOLOGY RECONSTRUCTION USING FUZZY-LOGIC DETECTION AND BAYESIAN TRACING ALGORITHMS

Miroslav Radojević, Ihor Smal, Erik Meijering

Biomedical Imaging Group Rotterdam
Erasmus University Medical Center, Rotterdam, the Netherlands
Email: m.radojevic@erasmusmc.nl

ABSTRACT

Digital reconstruction of neuronal cell morphology from microscopy image data is an important task in many neuroscience studies. Since the quality of the images is typically low due to noise, imperfect staining, or uneven illumination, and the morphology of neurons can be very complex, reconstruction is often very challenging even for expert human annotators. Many (semi)automatic reconstruction methods have been proposed in recent years, but they are far from perfect, and the challenge remains to develop better methods. Here we introduce a new fully automatic neuron reconstruction method that combines fuzzy-logic based detection of critical points in the images and Bayesian probabilistic tracing between these points. The method was tested on 2D fluorescence microscopy images of real single neurons with corresponding manual annotations. Our method proves to be more accurate (smaller median error) and substantially more robust (smaller error variance) compared to an alternative state-of-the-art method based on all-path pruning.

Index Terms—Neuron reconstruction, Bayesian filtering, fuzzy logic, fluorescence microscopy.

1. INTRODUCTION

Studies of the anatomy and function of neuronal cells and networks rely on accurate quantitative descriptions of the axonal and dendritic trees extracted from microscopy image data. Statistical analyses of parameters such as the length of the branches or their spatial distribution computed from these descriptions may provide answers to important research questions [1]. Because of the sheer volume of the image data in typical experiments, such analyses are possible at large only if the neuron morphology can be faithfully reconstructed fully automatically. This task has been a challenge for many years [2, 3] and is commonly hampered by ambiguities due to the low quality of the images and the high complexity of the neuronal arborizations. In a recent competition [4] many advanced neuron reconstruction methods

were compared in a praiseworthy attempt to accelerate the progress in the field and to bridge the gap between algorithmic supply by computer scientists and practical demand in neuroscience. Nonetheless, neuroanatomists tend to agree that current state-of-the-art methods for neuron reconstruction are not yet versatile and robust enough to fully substitute the human expert, and that many challenges remain [5], requiring the development of improved solutions.

In this paper we propose a novel solution for fully automatic reconstruction of neuron morphology from microscopy images. The method first detects the junction and end point regions of the tree structure and then employs sequential Bayesian filtering to trace the segments in between the critical point regions to construct the final tree. The position and size of the critical point regions is calculated using a fuzzy-logic system that applies a set of effective classification rules, and a mean-shift algorithm that clusters the directions of the image structures forming each critical point region. Together these features provide a guidance landmark map for the Bayesian tracing algorithm. Here we briefly describe our method and present experimental results showing its performance for real 2D fluorescence microscopy images of single neurons, using expert manual tracing as the gold standard. We also present a comparison with a recently proposed automatic neuron tracing method based on all-path pruning [6], the results of which clearly demonstrate the improvement of our method over the current state of the art.

2. METHOD

The proposed method consists of two essential steps (Fig. 1): 1) detecting and characterizing critical point regions, specifically junctions and end points, and 2) connecting these regions by tracing elongated image structures and aggregating the traces into a tree representation.

2.1. Critical Point Region Detection

For our purposes, critical point (CP) regions are defined as image regions where three or more elongated structures join (junctions), or regions where such structures terminate (end

This work was funded by the Netherlands Organization for Scientific Research (NWO grant 612.001.018 awarded to EM).

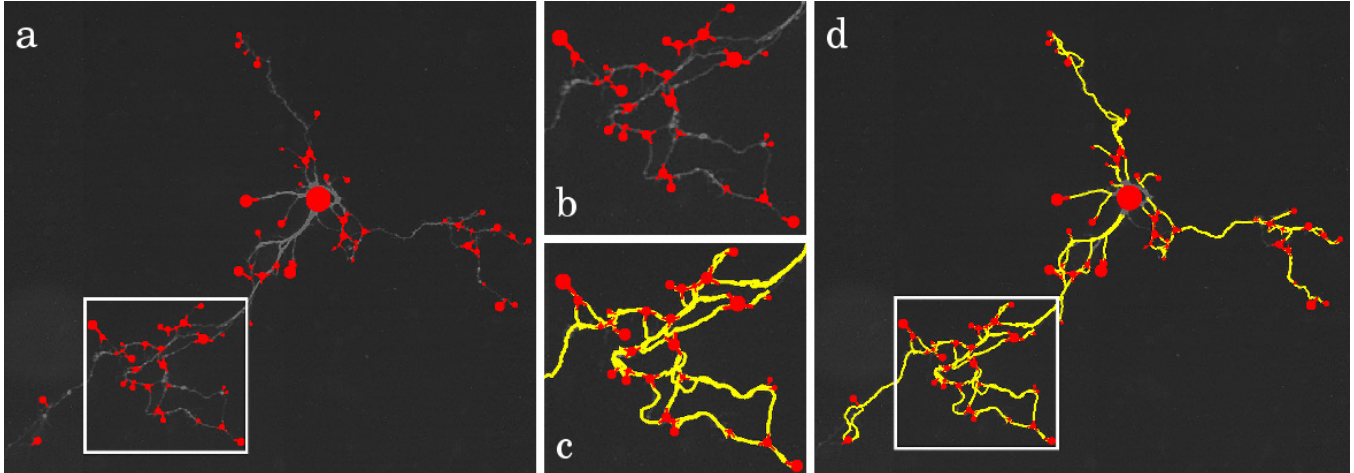


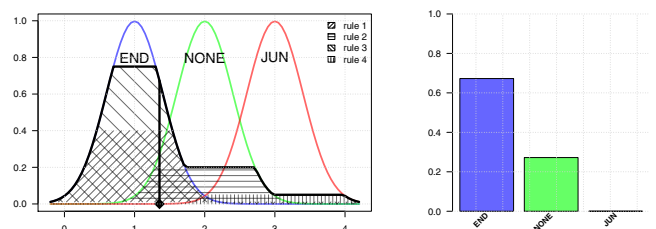
Fig. 1. Method outline: (a) Original image (822x678 pixels) with detected junction and end point regions. (d) Sequential Bayesian filtering result connecting the critical points. (b,c) Zooms of the regions indicated in (a) and (d), respectively.

points). To detect both types of regions, and to correctly classify them, we have extended our recent work on bifurcation detection [7]. In short, Gaussian directional filtering is performed at every pixel location to extract the key directions and corresponding centerline estimates as local intensity maxima of the local image structures. The filter responses and the bending energy of the local centerlines are fed to a fuzzy-logic rule-based system that outputs the degree of membership (in the range $[0,1]$) to the fuzzy sets JUN (junction), END (end point), or NONE (no CP) (Fig. 2a). Connected pixels of high membership degrees for JUN or END are clustered to form the set of CP regions (Fig. 2b). For each CP region, the main directions of the local elongated image structures connecting to that region are found by applying mean-shifting [8] to the pixel-wise direction estimates (Fig. 2c). The soma (cell body) of the neuron, being a special CP, is usually the brightest and largest connected region in the image and can therefore be easily extracted based on intensity and size.

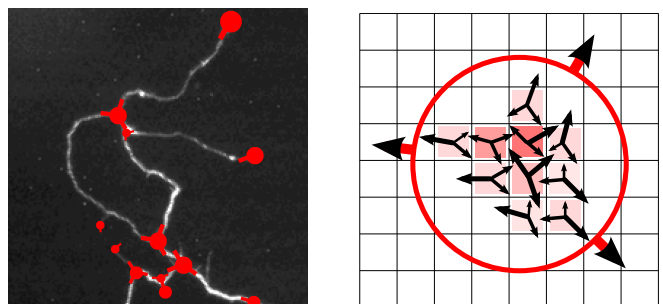
2.2. Bayesian Sequential Tracing

Methods for neuron tracing typically employ shortest-path algorithms or fast-marching based energy minimization to connect relevant pixels [2, 3]. The former require combinatorial analysis to form the tree from given landmark points, whereas the latter gradually build up the tree while keeping track of potential critical points, and both may require retrospective tree pruning. Here we propose an alternative solution for neuron tracing based on Bayesian sequential filtering.

The basic idea is to estimate a sequence of hidden states $\mathbf{x}_{0:L} = (\mathbf{x}_0, \dots, \mathbf{x}_L)$, in our case representing a dendritic or axonal path, using a set of measurements $\mathbf{y}_{0:L}$ along the path in the image \mathcal{I} . Here, the state is defined as $\mathbf{x} = (\mathbf{p}, \mathbf{v}, I)$, where $\mathbf{p} = (x, y)^T$ is the spatial location, $\mathbf{v} = (v_x, v_y)^T$ is the orientation of the path segment at that location, and I is the intensity of the segment. Both \mathbf{x}_0 and \mathbf{x}_L represent CP



(a) Fuzzy set membership degrees for an example case.



(b) Detected CP regions.

(c) Main CP directions.

Fig. 2. Detection of the critical point (CP) regions.

regions, where the trace begins and ends, respectively. By means of Bayes' theorem, it is possible to recursively compute the posterior distribution $p(\mathbf{x}_{0:L}|\mathbf{y}_{0:L})$ of the path $\mathbf{x}_{0:L}$, having all the measurements $\mathbf{y}_{0:L}$, as

$$p(\mathbf{x}_{0:L}|\mathbf{y}_{0:L}) = p(\mathbf{x}_0) \prod_{i=1}^L p(\mathbf{y}_i|\mathbf{x}_i)p(\mathbf{x}_i|\mathbf{x}_{i-1}) \quad (1)$$

assuming the transition prior $p(\mathbf{x}_i|\mathbf{x}_{i-1})$ is Markovian and the measurement \mathbf{y}_i depends only on the state \mathbf{x}_i . Starting from \mathbf{x}_0 , the filtering procedure recursively makes predictions according to $p(\mathbf{x}_i|\mathbf{x}_{i-1})$ and corrects them using the measurement \mathbf{y}_i and the likelihood $p(\mathbf{y}_i|\mathbf{x}_i)$.

In practice, for computational reasons, the posterior is approximated with N weighted samples $\{\mathbf{x}_{0:L}^k, w_L^k\}_{k=1}^N$ as $p(\mathbf{x}_{0:L}|\mathbf{y}_{0:L}) \approx \sum_k w_L^k \delta(\mathbf{x}_{0:L} - \mathbf{x}_{0:L}^k)$, where $\sum_k w_L^k = 1$. To adequately sample the state space, at each iteration i , we predict N new states \mathbf{x}_i^k and update their weights w_i^k . Each previous state \mathbf{x}_{i-1}^k contributes with N_k predictions, proportional to w_{i-1}^k such that $\sum_k N_k = N$, by distributing them on a semi-circular wavefront at distance D (Fig. 3a). In our application we use $N_k = \lfloor w_{i-1}^k N + \frac{1}{2} \rfloor$. For all $k \in \{1, \dots, N\}$ the components of the state vector are propagated as

$$\mathbf{p}_i^m = \mathbf{p}_{i-1}^k + D\mathbf{v}_{i-1}^k e^{j\frac{\pi}{2}\left(\frac{2(m-1)}{N_k-1}-1\right)} \quad (2)$$

$$\mathbf{v}_i^m = \mathbf{v}_{i-1}^k e^{j\frac{\pi}{2}\left(\frac{2(m-1)}{N_k-1}-1\right)} \quad (3)$$

$$I_i^m = I_{i-1}^k \quad (4)$$

where $m \in \{1, \dots, N_k\}$ indexes the predictions from the state sample indexed with k . The transition prior $p(\mathbf{x}_i|\mathbf{x}_{i-1})$ weights each prediction based on the angular divergence from \mathbf{v}_{i-1}^k in the dynamics model as

$$\tilde{w}_i^k = \exp\left(-\frac{1}{2\sigma_\alpha^2}\left(\frac{(m-1)\pi}{N_k-1} - \frac{\pi}{2}\right)^2\right) \quad (5)$$

where σ_α^2 parametrizes the angular divergence variance. The likelihood $p(\mathbf{y}_i|\mathbf{x}_i)$ represents the weight assigned to the states with respect to the corresponding image intensity $\mathcal{I}(\mathbf{p}_i^k)$ and, simultaneously, the similarity with the predicted intensity I_i^k at \mathbf{p}_i^k . It is used to update the weights as

$$w_i^k \propto p(\mathbf{y}_i|\mathbf{x}_i^k)\tilde{w}_i^k = \tilde{w}_i^k \mathcal{I}(\mathbf{p}_i^k) \exp\left(-\frac{(\mathcal{I}(\mathbf{p}_i^k) - I_i^k)^2}{2\sigma_I^2}\right) \quad (6)$$

where σ_I^2 parametrizes the intensity difference variance. After the update (6) the weights are normalized. The final path estimate is computed with subpixel accuracy from the weighted samples as a centroid: $\hat{\mathbf{x}}_{0:L} = \sum_k w_L^k \mathbf{x}_{0:L}^k$.

The proposed tracing scheme commences from the CPs, which are processed sequentially. Each CP initializes a number of tracings, depending on the number of main directions found in the detection stage (Fig. 3b), and each tracing ends if another CP is reached (Fig. 3c) or an intensity drop is detected between segment lengths of W pixels along the found path. Finally, the found traces are examined for overlap and added to a tree representation of the neuron.

3. RESULTS

The method was implemented in Java as a plugin for the open-source image analysis platform ImageJ. The key user parameters of the CP detection stage are the directional filter kernel size, which corresponds to the scale of the CP regions in the image, and the fuzzification parameters, as described previously [7]. The key user parameters of the tracing stage are the

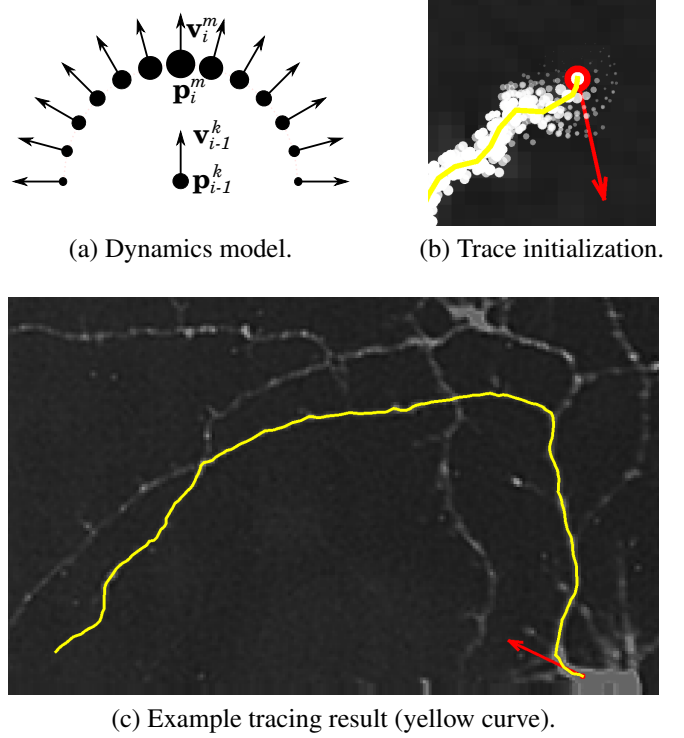


Fig. 3. Bayesian sequential tracing.

step size D reflecting the expected neurite diameter (typically 4-6 pixels), the standard deviation of the angular divergence σ_α (typically 30-50 degrees) and of the intensity difference σ_I (fixed at 25% of the effective dynamic range), and the intensity averaging range W (typically 10 pixels). The number of samples N is chosen so that the arc of radius D is sampled sufficiently ($N = 50$ in our experiments).

As a preliminary evaluation we tested our method on 19 real 2D fluorescence microscopy images of single neurons from a previous study [9]. Tracing results were evaluated against gold-standard reconstructions obtained using the manual annotation and correction functionality of Vaa3D [10]. Dissimilarity was expressed as the spatial distance (SD), substantial SD (SSD), and the percentage of sample points used in SSD (%SSD), as defined previously [10]. The results are presented in Table 1. For visual interpretation of these results, example reconstructions (corresponding to low, medium, and high values of SD) are shown in Fig. 4.

To assess the performance of our method compared to the state of the art, we also applied the recently proposed APP2 reconstruction method based on all-path pruning [6], available as a plugin of Vaa3D [10]. The parameter settings of both methods were optimized for best performance. Boxplots summarizing the SD, SSD, and %SSD scores of our method and APP2 for the 19 test images and corresponding gold-standard reconstructions are shown in Fig. 5. We conclude that our method yields a small but consistent improvement according to the median of all three measures, with a significantly reduced variance of the reconstruction errors.

| | #1 | #2 | #3 | #4 | #5 | #6 | #7 | #8 | #9 | #10 | #11 | #12 | #13 | #14 | #15 | #16 | #17 | #18 | #19 |
|------|-------|-------|-------|-------|-------|-------|-------|-------|-------|-------|-------|-------|-------|-------|-------|-------|-------|-------|-------|
| SD | 8.41 | 3.86 | 4.48 | 3.60 | 1.89 | 8.70 | 4.89 | 14.32 | 4.14 | 2.44 | 5.41 | 2.66 | 1.73 | 4.99 | 4.50 | 3.95 | 1.76 | 5.19 | 8.07 |
| SSD | 32.74 | 23.34 | 18.87 | 15.22 | 18.38 | 25.91 | 22.38 | 51.33 | 18.56 | 12.33 | 18.58 | 13.76 | 12.56 | 22.32 | 20.21 | 21.35 | 13.78 | 25.82 | 34.72 |
| %SSD | 0.22 | 0.10 | 0.15 | 0.14 | 0.05 | 0.26 | 0.13 | 0.17 | 0.14 | 0.09 | 0.16 | 0.11 | 0.05 | 0.14 | 0.15 | 0.13 | 0.05 | 0.16 | 0.16 |

Table 1. Dissimilarity between the obtained reconstructions and the gold-standard reconstructions for the 19 test images.

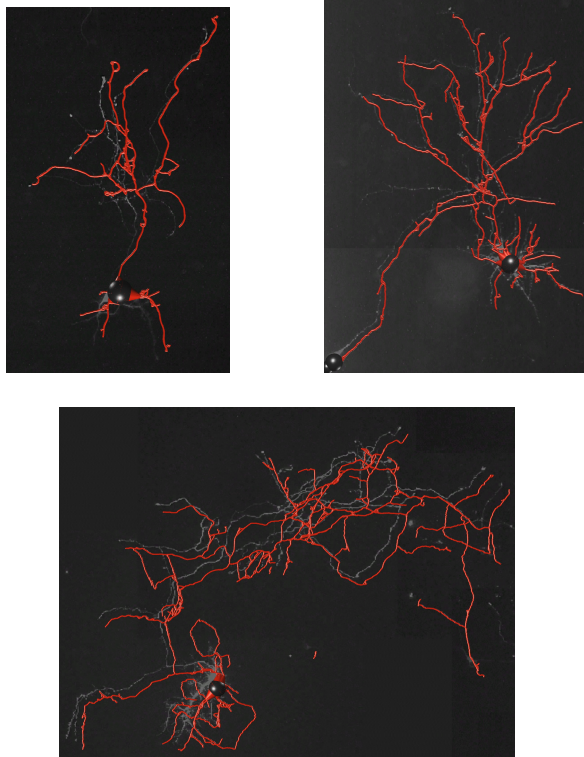


Fig. 4. Examples of neuron reconstructions with our method. The reconstructions (in red) are slightly displaced with respect to the image to facilitate visual comparison. The upper row contains reconstructions of neurons #13 (left) and #9 (right), and the bottom row shows neuron #8 (Tab. 1). These examples cover the range of SSD dissimilarity scores.

4. DISCUSSION

We have presented a new method for neuron morphology reconstruction in fluorescence microscopy images. The method is a fusion of two complementary algorithms that aim to solve two different aspects of the neuron reconstruction problem: the detection of critical points (specifically junctions and end points) and the subsequent tracing of the intermediate elongated image structures. The first algorithm is an extension of our recent work [7] and the second algorithm is entirely novel and is based on a Bayesian estimation approach that to the best of our knowledge has never been used before for neuron tracing. The method has been tested on real image data and the results show a clear improvement compared to a state-of-the-art method [6] that does not use explicit prior detection of critical points. In this work we have limited ourselves to 2D

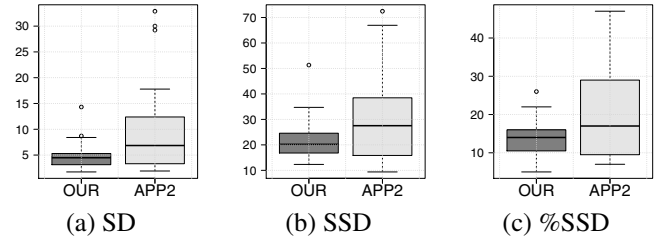


Fig. 5. Comparison of our method with APP2 using boxplots (in the R software package) of the results.

image data as this reflects the vast majority of neurobiological experiments. Future work will include extension to 3D, improved handling of overlapping traces to avoid redundant reconstructions, and more extensive evaluation involving not only more images but also additional performance measures scoring topological aspects of the reconstructions.

5. REFERENCES

- [1] M. Halavi, K. A. Hamilton, R. Parekh, and G. A. Ascoli, “Digital reconstructions of neuronal morphology: three decades of research trends,” *Frontiers in Neural Circuits*, vol. 6, no. 49, pp. 1–11, 2012.
- [2] E. Meijering, “Neuron tracing in perspective,” *Cytometry Part A*, vol. 77, no. 7, pp. 693–704, 2010.
- [3] D. E. Donohue and G. A. Ascoli, “Automated reconstruction of neuronal morphology: an overview,” *Brain Research Reviews*, vol. 67, no. 1, pp. 94–102, 2011.
- [4] T. A. Gillette, K. M. Brown, K. Svoboda, Y. Liu, and G. A. Ascoli, “DI-ADeMchallenge.Org: a compendium of resources fostering the continuous development of automated neuronal reconstruction,” *Neuroinformatics*, vol. 9, no. 2-3, pp. 303–304, 2011.
- [5] Y. Liu, “The DIADEM and beyond,” *Neuroinformatics*, vol. 9, no. 2-3, pp. 99–102, 2011.
- [6] H. Xiao and H. Peng, “APP2: automatic tracing of 3D neuron morphology based on hierarchical pruning of a gray-weighted image distance-tree,” *Bioinformatics*, vol. 29, no. 11, pp. 1448–1454, 2013.
- [7] M. Radojević, I. Smal, W. Niessen, and E. Meijering, “Fuzzy logic based detection of neuron bifurcations in microscopy images,” in *Proceedings of the IEEE International Symposium on Biomedical Imaging*. IEEE, April 2014, pp. 1307–1310.
- [8] Y. Cheng, “Mean shift, mode seeking, and clustering,” *IEEE Transactions on Pattern Analysis and Machine Intelligence*, vol. 17, no. 8, pp. 790–799, 1995.
- [9] P. Steiner, J.-C. F. Sarria, B. Huni, R. Marsault, S. Catsicas, and H. Hirling, “Overexpression of neuronal Sec1 enhances axonal branching in hippocampal neurons,” *Neuroscience*, vol. 113, no. 4, pp. 893–905, 2002.
- [10] H. Peng, Z. Ruan, F. Long, J. H. Simpson, and E. W. Myers, “V3D enables real-time 3D visualization and quantitative analysis of large-scale biological image data sets,” *Nature Biotechnology*, vol. 28, no. 4, pp. 348–353, 2010.